# Laser patterning and crystallization of 2D materials on rigid and flexible substrates

Zabihollah Ahmadi<sup>1</sup>, Parvin Fathi-Hafshejani<sup>1</sup>, Masoud Mahjouri-Samani <sup>1\*</sup>

<sup>1</sup>Electrical and Computer Engineering Department, Auburn University, Auburn, AL 36849, USA.

\*Address correspondence to: mahjouri@auburn.edu

#### **ABSTRACT**

Two-dimensional (2D) materials have been viewed as a promising candidate for future electronic, optoelectronic, and photonic applications. This, however, demands controlled synthesis and precise integration of such materials with complex patterns onto rigid and flexible substrates. Here we introduce a new laser-based approach that enables the integration of 2D materials onto the flexible and rigid substrate with desired shapes and patterns. We report direct laser crystallization and the pattering of MoS<sub>2</sub> and WSe<sub>2</sub> on PDMS. A thin layer of solid-state stoichiometric amorphous 2D film is deposited onto the substrates, followed by a controlled crystallization and direct writing process using a tunable nanosecond laser (1064 nm). This novel method enables the use of emerging 2D materials in future electronics, optoelectronics, and photonics applications where intricate patterning on rigid and flexible substrates are required.

**Keywords:** 2D materials, flexible nanoelectronics, additive nanomanufacturing, laser processing, direct patterning

### 1. INTRODUCTION

The recent growth of wearable functional devices indicates that printed electronics will be one of the future technology's major players (IoT). Printed electronics on rigid and flexible substrates have growing applications in various scientific and technological fields such as energy and storage, consumer electronics, healthcare, and defense. For such applications, it is crucial to integrate various electronic materials, including metals, insulators, semiconductors, and other emerging multifunctional and quantum materials with unique properties. Layered crystalline materials with intralayer covalent bonding and interlayer Van der Waals bonding, also known as two-dimensional (2D) quantum materials, are one of the promising candidates to fulfill such applications due to unique electrical, mechanical, and optical properties. For instance, compared to the organic, amorphous, metal oxide, polysilicon, and other semiconducting materials, large bandgap transition metal dichalcogenides (TMDCs) show mobility near to single-crystal silicon while they have a lower thickness and higher strain limits. [11-14]

Exfoliation and transfer from bulk materials or samples grown by, for example, chemical vapor deposition (CVD) method, are conventional synthesis and growth method to place crystalline 2D TMDCs onto various rigid or flexible substrates, especially the one that can not tolerate high temperatures for direct growth of 2D crystals on them.<sup>[15-18]</sup> Size uniformity, uncontrolled nanosheet orientations, and contamination between layers are some of the challenges that hinder these methods

to be the main manufacturing techniques of 2D materials for such applications. To synthesis crystalline 2D TMDCs directly onto the substrates, the synthesis temperatures typically range between 650 to 850 °C. However, most glasses and flexible substrates such as BK7, polydimethylsiloxane (PDMS), polyethylene terephthalate (PET), and polyimides cannot withstand such high growth temperatures and will be deformed or damaged. Next-generation printing of functional materials and flexible devices demands suitable and efficient processes. The traditional lithography process is time-consuming and costly that includes toxic solvents and strong acids, and needs multiple processing steps.<sup>[19]</sup> Inkjet printing of 2D materials has been proposed as a promising patterning method. However, contaminant-free and uniform patterning of inkjet printing is still challenging. In addition, inkjet printing requires toxic solvents and additives that add further complexity to the ink manufacturing and printing process.<sup>[20-22]</sup>

Here, we report a controlled patterning and crystallization of 2D materials directly on rigid and flexible substrates via a tunable nanosecond fiber laser without damaging the underlying substrates. Thin layers of stoichiometric amorphous 2D quantum materials were first pulsed laser deposited onto the substrates. These amorphous films were then placed inside an environmental chamber in an argon environment and at room temperature to perform controlled laser crystallization and patterning. We show that 2D crystals can be formed by tuning the pulse duration, the number of pulses, scan speed, and laser power. The pulsed nanosecond laser coupled to a galvo scanner was used for programmable patterning of 2D crystals. This photo-selective crystallization and patterning method resulted in a controlled and uniform formation of 2D crystals on different substrates.

## 2. EXPERIMENTAL SETUP

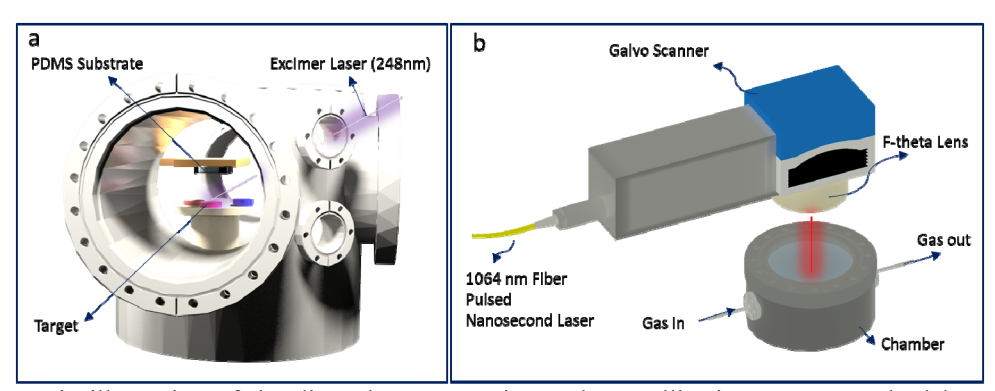


Figure 1. Schematic illustration of the direct laser patterning and crystallization process. Pulsed laser deposition of amorphous 2D films (a), laser patterning, and crystallization (b).

In this work, molybdenum disulfide (MoS<sub>2</sub>) and tungsten diselenide (WSe<sub>2</sub>) materials were chosen due to their broad range of applications. As shown in Figure 1, the experimental setup comprises a pulsed laser deposition (PLD) system, a tunable fiber nanosecond laser (1064 nm), a galvo scanner, and a home-built environmental chamber. A pulsed laser deposition system was first utilized to additively deposit stoichiometric amorphous 2D films (MoS<sub>2</sub> or WSe<sub>2</sub>) onto the rigid and flexible substrates (Figure 1a). An excimer laser with 248 nm wavelength was used to ablate the MoS<sub>2</sub> and WSe<sub>2</sub> targets with 5 Hz repetition rate. The laser spot size, fluence, deposition pressure, and substrates-target distance were  $2 \times 5$  mm, 1.5 J cm<sup>-2</sup>,  $\sim 5 \times 10^{-7}$  Torr,  $\sim 7$  cm, respectively. Once the desired amorphous 2D film formed, substrates were then placed into the environmental chamber for

laser processing and patterning. A pulsed nanosecond fiber laser with tunable pulse duration, repetition rate, and power was coupled to a galvo scanner head (Figure 1b) to precisely pattern 2D crystals with around 15  $\mu$ m line resolution and a  $7\times7$  cm<sup>2</sup> work field. Laser crystallization and patterning was performed at an atmospheric argon environment with a 200 sccm flow rate to avoid surface oxidation during the crystallization and patterning process. The laser repetition rate and power were fixed at 100 KHz, and 26 W for processing on PDMS and 1 MHz and 78 W for laser processing on silica.

#### 3. RESULTS AND DISCUSSION

The thickness of amorphous 2D films deposited by the PLD system can be controlled by the deposition time or the number of PLD pulses, as showing in Figure 2a. The interaction of 1064 nm laser with the amorphous layer decreases midgap and defect states of amorphous 2D films and will result in crystallization of 2D film. As shown in Figure 2b, we observed that longer pulse duration and less number of laser pulses is required for crystallization and vice versa. For example, 197 ns pulse duration will result in the evaporating of the amorphous WSe<sub>2</sub>/PDMS regardless of the number of laser pulses, while good crystallization of WSe<sub>2</sub> will observe after the first 12 or 14 pulses of laser with 80 ns pulse duration. By increasing the number of the pulses from 14 to 16 while the pulse duration is still unchanged (80 ns), the WSe<sub>2</sub> film was evaporated from the PDMS substrate. This indicates the low thermal conductivity of both the PDMS substrate and the amorphous 2D film. Therefore, 1064 nm pulsed nanosecond laser enables crystallization in a time-resolved process by precisely controlling the amount of laser energy interacted with the amorphous 2D layers. Silica as a transparent substrate has higher thermal conductivity, and heat dissipates quicker in silica compared to PDMS. As a result, crystallization will happen at 261 ns and 20 pulses. Figure 2c,d shows the evaporated and crystallized MoS<sub>2</sub> deposited on silica. Raman map shown in the inset of Figure 2d demonstrates the spatial uniformity of crystallized MoS<sub>2</sub> on silica.

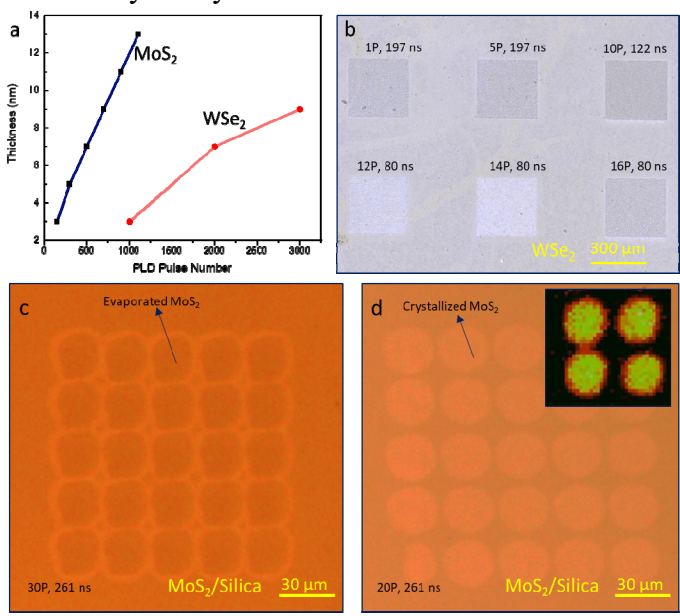


Figure 2. The thickness of PLD-deposited  $WSe_2$  and  $MoS_2$  films as a function of pulse number (a). Optical images of a 7 nm  $WSe_2$  on PDMS substrate (b), evaporated  $MoS_2$  (c) and crystallized  $MoS_2$  on fused silica (d). The inset image is the Raman map of the crystallized  $MoS_2$  dots on fused silica.

Raman spectra of the amorphous and crystallized MoS<sub>2</sub> layers at different pulse durations and pulse numbers were obtained to characterize the patterned 2D materials. As shown in Figure 3a, direct laser processing resulted in the appearance of Raman peaks at ~375 cm<sup>-1</sup> and ~405 cm<sup>-1</sup> showing the crystallinity of 2D MoS<sub>2</sub> layers. By increasing the pulse numbers, the intensity of the Raman peaks increased, and peaks got sharper and narrower, suggesting the increased quality of the crystallized MoS<sub>2</sub>. As Figure 3b shows, the Raman spectrum of PLD-deposited MoS<sub>2</sub> did not have any peaks, which indicates the amorphous nature of the deposited 2D layers. Once the number of pulses reached a certain number, the MoS<sub>2</sub> started evaporating from the PDMS substrate (red spectrum in Figure 3b).

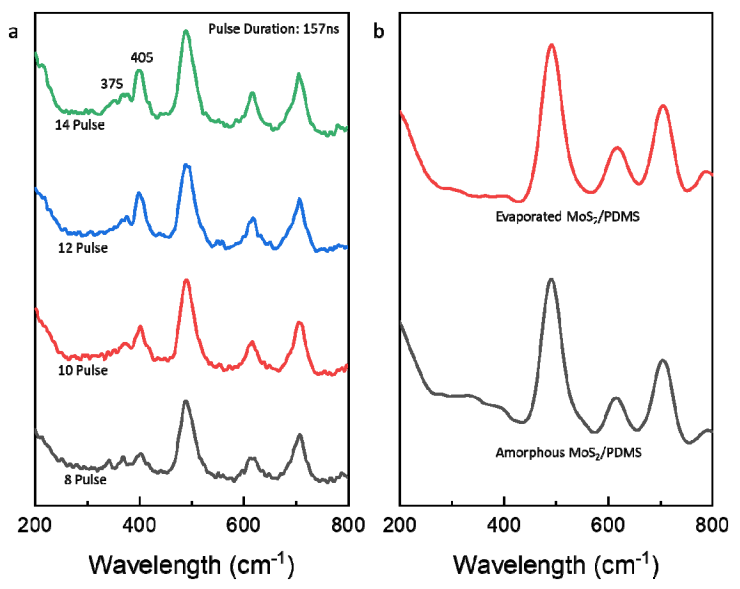


Figure 3. Raman spectra of crystallized MoS<sub>2</sub>/PDMS using different pulse numbers (a) at 157 ns pulse duration (power=26W), and the PLD-deposited MoS<sub>2</sub>/PDMS (black spectrum), evaporated MoS<sub>2</sub>/PDMS (red spectrum) in (a).

To further assess direct laser crystallization ability in patterning complex shapes, we crystallized the as-PLD deposited amorphous MoS<sub>2</sub> films on the PDMS substrates, as shown in Figure 4. The darker areas are the amorphous MoS<sub>2</sub> film, while the brighter lines show the laser-transferred amorphous to the crystalline phase. Additionally, this method shows that it could be scaled up to larger areas.

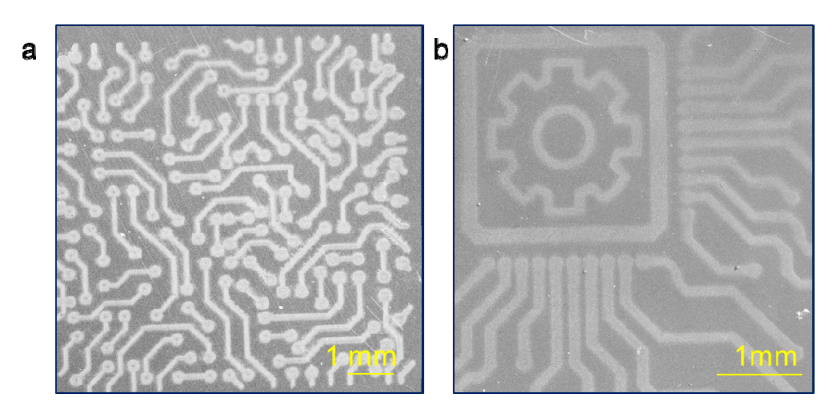


Figure 4. Optical image of crystallized MoS<sub>2</sub> patterns via nanosecond laser.

Figure 5 shows the laser process parameters (pulse duration, number of pulses) where the transformation of amorphous 2D MoS<sub>2</sub> and WSe<sub>2</sub> to crystalline phases were obtained. For example, employing 12 pulses of laser with 157 ns pulse duration on a 3 nm PLD-deposited MoS<sub>2</sub> resulted in crystallization of 2D films. Color-shaded areas show the laser processing window, which results in an acceptable crystallization outcome. Laser parameters outside these regions resulted in either evaporation of 2D films (to the right of the line) or no effect (to the left of the line). Therefore, the laser process parameters above the color-shaded areas could also be employed for selective evaporation of the unwanted 2D films from the substrates.

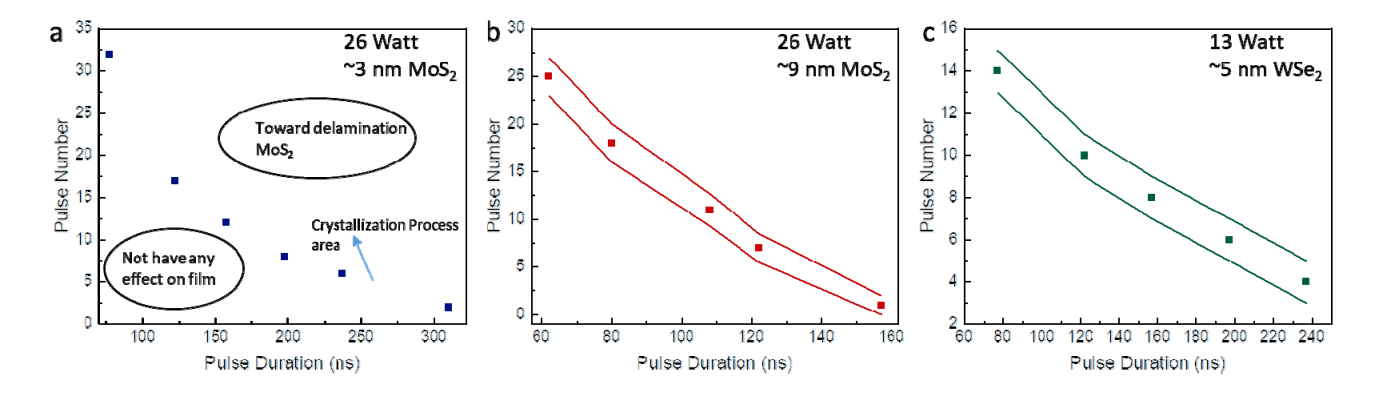


Figure 5. Effect of laser pulse duration and pulse number on the crystallization of amorphous layers of  $\sim$ 3 nm MoS<sub>2</sub> (a),  $\sim$ 9 nm MoS<sub>2</sub> (b), and  $\sim$ 5 nm WSe<sub>2</sub> (c).

### 4. CONCLUSION

In summary, we showed that the nanosecond pulsed laser interaction with the amorphous 2D MoS<sub>2</sub> and WSe<sub>2</sub> films deposited onto the rigid and PDMS substrates by the PLD process resulted in the crystallization of the 2D film without impacting the underlying substrates. Despite the low optical absorption of PDMS, the low thermal conductivity of the PDMS substrate would result in the evaporation of deposited amorphous 2D materials by lasers. Therefore, we showed that a 1064 nm pulse nanosecond laser could crystallize 2D materials, deposited onto both rigid and flexible substrates, in a controlled process. Different pulse durations and pulse numbers can be employed to obtain high quality crystallized 2D layers. We further showed coupling a pulsed nanosecond laser to a galvo scanner head enables direct patterning and crystallization of 2D TMDCs such as MoS<sub>2</sub> and WSe<sub>2</sub>.

#### 5. ACKNOWLEDGMENTS

This research is partially funded by the US National Science Foundation (NSF) (grant No. 1923363).

#### REFERENCES

- 1. Liang, Z., et al., Flexible lead-free oxide film capacitors with ultrahigh energy storage performances in extremely wide operating temperature. Nano Energy, 2019. 57: p. 519-527.
- 2. Spanu, A., et al., Flexible and wearable monitoring systems for biomedical applications in organic flexible electronics: Fundamentals, devices, and applications, in Organic Flexible Electronics. 2021. p. 599-625.
- 3. Tinoco, J.C., et al., *Fabrication of Schottky barrier diodes based on ZnO for flexible electronics*. Journal of Materials Science: Materials in Electronics, 2020. **31**(10): p. 7373-7377.
- 4. Ma, Y., et al., Flexible Hybrid Electronics for Digital Healthcare. Advanced Materials, 2019. 32(15).
- 5. Rohaizad, N., et al., *Two-dimensional materials in biomedical, biosensing and sensing applications.* Chemical Society Reviews, 2021. **50**(1): p. 619-657.
- 6. Zhu, W., et al., Advancements in 2D flexible nanoelectronics: from material perspectives to RF applications. Flexible and Printed Electronics, 2017. **2**(4).
- 7. Glavin, N.R., C. Muratore, and M. Snure, *Toward 2D materials for flexible electronics: opportunities and outlook.* Oxford Open Materials Science, 2021. **1**(1).
- 8. Azam, N., et al., Accelerated synthesis of atomically-thin 2D quantum materials by a novel laser-assisted synthesis technique. 2D Materials, 2019. 7(1).
- 9. Ahmadi, Z., et al., *Application of lasers in the synthesis and processing of two-dimensional quantum materials.* Journal of Laser Applications, 2019. **31**(3).
- 10. Ahmadi, Z., et al., *Self-limiting laser crystallization and direct writing of 2D materials*. International Journal of Extreme Manufacturing, 2019. **1**(1).
- 11. Akinwande, D., N. Petrone, and J. Hone, *Two-dimensional flexible nanoelectronics*. Nature Communications, 2014. **5**(1).
- 12. Yu, J., et al., Designing the Bending Stiffness of 2D Material Heterostructures. Advanced Materials, 2021.
- 13. Georgiou, T., et al., Vertical field-effect transistor based on graphene–WS2 heterostructures for flexible and transparent electronics. Nature Nanotechnology, 2012. 8(2): p. 100-103.
- 14. Li, J., N.V. Medhekar, and V.B. Shenoy, *Bonding Charge Density and Ultimate Strength of Monolayer Transition Metal Dichalcogenides*. The Journal of Physical Chemistry C, 2013. **117**(30): p. 15842-15848.
- 15. Coleman, J.N., et al., *Two-Dimensional Nanosheets Produced by Liquid Exfoliation of Layered Materials*. Science, 2011. **331**(6017): p. 568-571.
- 16. Kum, H.S., et al., *Heterogeneous integration of single-crystalline complex-oxide membranes*. Nature, 2020. **578**(7793): p. 75-81.
- 17. Kim, Y., et al., Remote epitaxy through graphene enables two-dimensional material-based layer transfer. Nature, 2017. **544**(7650): p. 340-343.
- 18. Chung, K., et al., growth and characterizations of GaN micro-rods on graphene films for flexible light emitting diodes. APL Materials, 2014. **2**(9).
- 19. Miyakawa, M., et al., Simple and reliable direct patterning method for carbon-free solution-processed metal oxide TFTs. Scientific Reports, 2018. **8**(1).
- 20. Carey, T., et al., Fully inkjet-printed two-dimensional material field-effect heterojunctions for wearable and textile electronics. Nature Communications, 2017. **8**(1).
- 21. Uzun, S., et al., Additive-Free Aqueous MXene Inks for Thermal Inkjet Printing on Textiles. Small, 2020. 17(1).
- 22. Zhang, C., et al., *Additive-free MXene inks and direct printing of micro-supercapacitors*. Nature Communications, 2019. **10**(1).